| | |
|---|---|
| Title | Sputtering of SiN films by 540 keV C^[2+]_[60] ions observed using high-resolution Rutherford backscattering spectroscopy |
| Author(s) | Nakajima, K.; Morita, Y.; Kitayama, T.; Suzuki, M.; Narumi, K.; Saitoh, Y.; Tsujimoto, M.; Isoda, S.; Fujii, Y.; Kimura, K. |
| Citation | Nuclear Instruments and Methods in Physics Research Section B: Beam Interactions with Materials and Atoms (2014), 332: 117-121 |
| Issue Date | 2014-08 |
| URL | http://hdl.handle.net/2433/188902 |
| Right | © 2014 Elsevier B.V. |
| Type | Journal Article |
| Textversion | author |

# Sputtering of SiN films by 540 keV $C_{60}^{2+}$ ions observed using high-resolution Rutherford backscattering spectroscopy

K. Nakajima[1], Y. Morita[1], T. Kitayama[1], M. Suzuki[1], K. Narumi[2], Y. Saitoh[2], M. Tsujimoto[3], S. Isoda[3], Y. Fujii[4] and K. Kimura[1*]

[1]Department of Micro Engineering, Kyoto University, Kyoto 615-8540, Japan

[2]Takasaki Advanced Radiation Research Institute, Japan Atomic Energy Agency, 1233 Watanuki-machi, Takasaki, Gumma 370-1292, Japan

[3]Institute for Integrated Cell-Material Sciences, Kyoto University, Kyoto 606-8501, Japan

[4]Center for Supports to Research and Education Activities, Kobe University, Kobe 657-8501, Japan

[*]e-mail: kimura@kues.kyoto-u.ac.jp

Amorphous silicon nitride films deposited on Si(001) were irradiated with 540 keV $C_{60}$ ions to fluences ranging from $2.5 \times 10^{11}$ to $1 \times 10^{14}$ ions/cm$^2$. The composition depth profiles of the irradiated samples were measured using high-resolution Rutherford backscattering spectroscopy. Both silicon and nitrogen in the film decrease rapidly with fluence. From the observed result the sputtering yields are obtained as 3900 ± 500 N atoms/ion and 1500 ± 1000 Si atoms/ion. Such large sputtering yield cannot be explained by either the elastic sputtering or the electronic sputtering, indicating that the synergy effect between the elastic sputtering and the electronic sputtering plays an important role.

1. Introduction

When insulator surfaces are bombarded with swift heavy ions, electronic excitation may cause large sputtering yields, sometimes more than ten thousand. This is called electronic sputtering and has been extensively studied [1 – 7]. The observed electronic sputtering yield is proportional to the power of the electronic stopping power with a material dependent exponent of 2 – 4 [2]. There are several models proposed to explain the electronic sputtering, e.g. Coulomb explosion model [8], shock wave model [9], pressure pulse model [10], and inelastic thermal spike (i-TS) model. Among these models, the i-TS model can describe the electronic sputtering quantitatively for a large number of materials [2, 3]. The i-TS model was originally developed to explain the formation of ion tracks. During the passage through the matter swift heavy ions lose their energy mainly by electronic excitation processes. A part of energy deposited to the electrons is gradually transferred to target atoms. The temperature of the atoms increases along the ion path and consequently ion tracks are formed when the temperature exceeds the melting point. The elevated temperature also enhances the sputtering yield via the surface evaporation. Because both track formation and the electronic sputtering can be explained by the same model, there should be a strong relation between track formation and electronic sputtering [11]. There are a number of studies on the track formation as well as the electronic sputtering. However, relatively small number of studies address the relation between the track formation and the electronic sputtering, especially the relation between the microscopic structures of ion tracks and the electronic sputtering.

Recently, we have observed ion tracks produced by sub MeV $C_{60}$ ions in thin amorphous silicon nitride (a-SiN) films using transmission electron microscopy (TEM) [12, 13]. Examples of the observed TEM images of the a-SiN film of 20 nm thickness irradiated with 540 keV $C_{60}^{2+}$ ions are shown in Fig. 1. The TEM images indicate that the ion track consists of a low density cylindrical core (typical diameter and length are ~ 4 and ~ 15 nm, respectively) surrounded by a high density shell. The tilt image indicates that the track is homogeneous along the length of the track (see Fig. 1(b)). The radial density profile of the track was derived from the image of high-angle annular dark field scanning transmission electron microscopy (HAADF-STEM). The derived profile showed a large density reduction in the core region (about 20% reduction at the core center) and a slight enhancement of density in the shell region (1 – 2% enhancement). This suggests a large number of atoms are emitted from the ion track which penetrates deep into the bulk down to ~ 15 nm, namely the sputtered atoms originate from rather deep positions along

the ion track. This is very different from the elastic sputtering where atoms are emitted mainly from the topmost surface layer. In addition, the sputtering yield estimated from the HAADF-STEM image is as large as ~ 3600, which is about two orders of magnitude larger than the estimated electronic sputtering yield. This suggests that there is a new mechanism to enhance the sputtering yield. However, because HAADF-STEM allows only semi-quantitative analysis It is highly desired to measure the sputtering yield using fully quantitative technique to see if the large sputtering yield estimated from the HAADF-STEM image is correct or not. It is also interesting to confirm whether the target atoms are really emitted from the deep region along the ion track as was suggested by TEM and HAADF-STEM. In this paper, we measured the composition depth profiles of a-SiN samples bombarded with 540 keV $C_{60}$ ions at various fluences using high-resolution Rutherford backscattering spectroscopy (RBS). High-resolution RBS allows quantitative analysis with an excellent depth resolution (sub-nm resolution at surface). We found that the composition is modified in the depth region corresponding to the ion track. It is also found that the sputtering yield is indeed very large as was estimated from the HAADF-STEM image. The origin of such a large sputtering yield is discussed in terms of the synergy effect between the nuclear and electronic stopping powers.

## 2. Experimental

A wafer of Si(001) with an a-SiN film of 30 nm deposited by low pressure chemical vapor deposition (LPCVD) was purchased from Silson Ltd. The nominal density of the a-SiN film is 3 g/cm$^3$. A beam of 540 keV $C_{60}^{2+}$ was produced by the 400-kV ion implanter at JAEA/Takasaki. The a-SiN/Si(001) samples of 1 × 1 cm$^2$ were irradiated with the $C_{60}^{2+}$ ion beam at normal incidence to fluences from 2.5 × 10$^{11}$ to 1 × 10$^{14}$ ions/cm$^2$. The beam was raster scanned over the sample (the scan area was 2 × 2 cm$^2$) and the typical beam current was about 5 nA. After irradiation, the samples were measured using high-resolution RBS at Kyoto University. The details of the high-resolution RBS measurement were described elsewhere [14]. Briefly, $He^+$ ions are produced by a Penning ion gauge type ion source and accelerated up to 400 keV by a Cockcroft Walton type accelerator. The produced ion beam was mass analyzed by an analyzing magnet. The selected $He^+$ beam was collimated to 2 × 2 mm$^2$ by two sets of rectangular shaped slit system and sent to a scattering chamber. The typical beam current was about 50 nA and the pressure of the scattering chamber was ~1 × 10$^{-6}$ Pa during the measurements. The He ions

scattered from the sample at a scattering angle $\theta \approx 75^{o}$ were energy analyzed by a 90º sector type magnetic spectrometer and detected by a one-dimensional position sensitive detector (1D-PSD) of 100 mm length (the energy window was 25% of the central energy). We measured both <111> channeling and random spectra for each samples. The incident angles for channeling and random measurements were 54.7º and 50.2º, respectively. During the random measurement the sample was continuously rotated around the surface normal keeping the angle of incidence constant.

## 3. Results and discussion

Figure 2 shows an example of the observed HRBS spectra for the virgin sample. The spectrum observed under <111> channeling conditions (circles) is shown together with the random spectrum (triangles). Both spectra show nitrogen signals from ~225 to ~260 keV. The nitrogen signals are seen more clearly in the channeling spectrum due to the reduction of the silicon signals. There are small peaks at ~ 241 keV and 275 keV, which correspond to carbon and oxygen atoms at the surface. From these spectra composition depth profiles were derived through spectrum simulations. The simulation code was developed for high-resolution RBS. It employs energy loss straggling formula given by Yang *et al* [15] and screened Rutherford cross sections, but neglects multiple scattering. Figure 3 shows the derived composition depth profiles. The concentrations of silicon and nitrogen are almost constant in the film, which are 47% and 53% for silicon and nitrogen, respectively, indicating that the film composition is Si-rich compared to the stoichiometric $Si_3N_4$. At the surface there are carbon atoms of $6 \times 10^{15}$ atoms/cm$^2$, which is attributed to a thin surface contamination layer consisting of hydrocarbon. Similar amount of surface carbon was observed for all irradiated samples. In addition to the surface carbon, there are also oxygen atoms of $4 \times 10^{15}$ atoms/cm$^2$ in the surface region. These oxygen atoms probably form a thin silicon oxide layer at the surface. The depth scale shown in the upper abscissa was estimated with the nominal density (3 g/cm$^3$). From the width of the trapezoidal nitrogen profile, the thickness of the a-SiN film is estimated to be 28 nm, which is in reasonable agreement with the nominal thickness of 30 nm.

Figure 4 shows some examples of the observed <111> channeling spectra of the irradiated samples together with the virgin sample. With increasing fluence the nitrogen signal decreases, especially around the leading edge at ~259 keV, and almost disappears at the fluence of $9.2 \times 10^{13}$ ions/cm$^2$. Concerning the silicon signal, a large broad peak appears at ~290 keV after irradiation and the peak

becomes larger with increasing fluence. This broad peak is attributed to the radiation damage induced in the interfacial region. Note that silicon yield at the surface (~ 320 keV) increases with fluence, indicating that the silicon concentration in the surface layer increases with fluence. Composition depth profiles of the irradiated samples were also derived from these measured spectra through spectrum simulations.

The composition depth profiles of the irradiated sample at $2.3 \times 10^{13}$ ions/cm$^2$ are compared with those of the virgin sample in Fig. 3. At this fluence, the surface is completely covered by the ion tracks. The interface between the a-SiN film and the substrate Si moves towards surface by ~10 nm, indicating that a substantial portion of the film was sputtered by the $C_{60}^{2+}$ bombardment. It is noteworthy that there is almost no change in the shape of the trailing edge of the nitrogen profile. This indicates that the surface roughening due to the $C_{60}^{2+}$ bombardment is rather small. Besides the thinning of the film, a pronounced change of the film composition is clearly seen especially in the surface region. The nitrogen concentration decreases down to zero and the silicon concentration increases up to 70 at.% at a depth $d$ ~ 3 nm. This indicates that preferential sputtering of nitrogen occurs by the $C_{60}^{2+}$ bombardment which results in the reduction of nitrogen concentration and the enhancement of silicon concentration as observed. The nitrogen deficient region extends from the surface down to ~ 14 nm, which is in good agreement with the observed track length (14.6 nm) [2]. This indicates that the track interior is really modified as was observed by TEM and HAADF-STEM. In addition to the change of the silicon and nitrogen concentrations, the oxygen concentration increases. The oxygen atoms exist mainly in the surface region and there is a correlation between the nitrogen reduction and oxygen incorporation. These oxygen atoms are presumably incorporated to stabilize the silicon dangling bonds created by the nitrogen reduction when the irradiated sample was taken out from the irradiation chamber.

Figure 5 shows the amounts of silicon and nitrogen atoms in the a-SiN film as a function of the fluence. These results were fitted by exponential functions and the fitting results are shown by dashed curves. The sputtering yields of silicon and nitrogen were estimated by the slope of these curves at zero fluence. The obtained sputtering yields are 3900 ± 500 N atoms/ion and 1500 ± 1000 Si atoms/ion. This is roughly in agreement with the number of deficient atoms in a single track estimated from the HAADF-STEM image, which is 2600 N atoms and 1000 Si atoms. The difference could be attributed to the semi-quantitative nature of the HAADF-STEM analysis and the error in the estimation of the fluence. Such a large sputtering yield cannot be explained in terms of the elastic sputtering. The sputtering yield of

a-SiN with bombardment of monoatomic C ions of the same velocity (i.e. 9 keV C ion) is estimated to be only ~ 1 using the SRIM code [16]. Neglecting the cluster effect the elastic sputtering yield for 540 keV $C_{60}^{2+}$ ions is thus estimated to be only ~ 60. Even if the sputtering yield is enhanced by the cluster effect by a factor of 6, which was observed for the sputtering of amorphous silicon bombarded with 540 keV $C_{60}^{2+}$ ions [17], the estimated elastic sputtering yield is one order of magnitude smaller than the observed sputtering yield.

The electronic sputtering yield of a-SiN bombarded with monoatomic swift heavy ions was measured by Arnoldbik *et al* [18]. The measured sputtering yield for 50 MeV $Cu^{16+}$ ions is 400 nitrogen atoms/ion at an incident angle of 7° with respect to the surface plane. If a simple cosine law is assumed, the sputtering yield at normal incidence is estimated to be ~50 N atoms/ion. This is much smaller than that we observed for 540 keV $C_{60}$ bombardment even though the electronic stopping power for 50 MeV $Cu^{16+}$ ion (10.0 keV/nm) is 1.4 times larger than that for 540 keV $C_{60}$ ion (7.3 keV/nm). This indicates that the observed large sputtering yield cannot be explained by the electronic sputtering. It is noteworthy that the a-SiN sample used in the reference 18 was prepared by the same technique, LPCVD, as was used in the preparation of the present samples.

Comparison between the surface craters produced by swift $C_{60}$ ions and monoatomic swift heavy ions was reported [19]. A single crystal surface of an amino acid, L-valine was bombarded with 23 MeV $C_{60}$ ions and 78.2 MeV $^{127}I$ ions and observed by AFM. Both ions produce craters but much larger craters (diameter 70 $\pm$ 5 nm and depth 11.7 ± 1.2 nm) were observed for the bombardment of 23 MeV $C_{60}$ than that for 78.2 MeV $^{127}I$ ions. The volume of the crater produced by 23 MeV $C_{60}$ is 540 ± 390 times larger than that of 78.2 MeV $^{127}I$ ions while the electronic stopping power for 23 MeV $C_{60}$ is only 3.8 times larger than that for 78.2 MeV $^{127}I$. It is known that the electronic sputtering yield is proportional to the power of the electronic stopping power with a material dependent exponent of 2 – 4 [2]. Using this empirical power law, the sputtering yield ratio is estimated to be 14.4 – 209, which is in agreement with the observed removed volume ratio 540 ± 390 within the experimental error, indicating that the observed gigantic craters may be explained in terms of the electronic sputtering. Different from these previous results, the present result for 540 keV $C_{60}^{2+}$ cannot be explained by the electronic sputtering as was mentioned above.

A possible explanation of the observed large sputtering yield for 540 keV $C_{60}^{2+}$ ions could be the synergy effect of the electronic and elastic sputtering. The synergy between the electronic and nuclear

energy losses plays an important role in the track formation process [20]. In the present case, the nuclear stopping power for 540 keV $C_{60}^{2+}$ ions in a-SiN is as large as 9.9 keV/nm while that for 50 MeV $Cu^{16+}$ ions is negligibly small (37 eV/nm). The target atoms are heated by the nuclear stopping power more efficiently in comparison with the electronic stopping power because the projectile energy can be directly transferred to the atoms by nuclear stopping. Thus the nuclear stopping power contributes to the surface evaporation more efficiently than the electronic stopping power. The i-TS model predicts that the electronic stopping power of 6.84 keV/nm (corresponding to 40 MeV Au ion) produces ion tracks of 4-nm radius in $SiO_2$, while tracks of the same size can be produced by the nuclear stopping power of 3.07 keV/nm (corresponding to 1 MeV Au ion) [20]. This means that the nuclear stopping power is more than twice efficient than the electronic stopping power for the track formation. This enhancement factor may be applicable also for the electronic sputtering because both processes are well described by the i-TS model. Using this enhancement factor the effective stopping power of the 540 keV $C_{60}$ ion is estimated to be 29.4 keV/nm (= 9.9 × 6.84/3.07 + 7.3), which is 3 times larger than the electronic stopping power of 50 MeV $Cu^{16+}$ ions. Using the empirical power law mentioned above, the sputtering yield for 540 keV $C_{60}$ ions is estimated to be $3^2$ - $3^4$ times larger than that for 50 MeV $Cu^{16+}$ ions, namely the estimated sputtering yield is 450 – 4050 N atoms/ion. This rough estimation is in reasonable agreement with the sputtering yield of 3900 ± 500 N atoms/ion observed by the present high-resolution RBS measurements. It should be noted that both the shock wave model and the pressure pulse model predict that the sputtering yield is proportional to the third power of the electronic stopping power [21]. Thus, these models cannot also explain the present large sputtering yield unless the synergy effect is taken into account.

## 4. Conclusion

We have measured the sputtering yield of a-SiN bombarded with 540 keV $C_{60}^{2+}$ ions using high-resolution RBS. The observed sputtering yields of N and Si are as large as 3900 ± 500 N atoms/ion and 1500 ± 1000 Si atoms/ion, respectively. The sputtering yield estimated using the SRIM code is at least one order of magnitude smaller than the observed result, indicating that the observed large sputtering yield cannot be explained in terms of the elastic sputtering. The observed sputtering yield was compared with the previous measurement of the electronic sputtering yield of a-SiN bombarded with 50 MeV $Cu^{16+}$ ions [17]. Although the electronic stopping power for 50 MeV $Cu^{16+}$ ion is 1.4 times larger than that for

540 keV $C_{60}^{2+}$ ions, the observed sputtering yield for 50 MeV $Cu^{16+}$ ions is almost two orders of magnitude smaller than that for 540 keV $C_{60}^{2+}$ ions. Thus neither the elastic sputtering nor the electronic sputtering explains the observed large sputtering yield, suggesting that the synergy effect plays an important role. A rough estimation of the synergy effect between the nuclear and electronic stopping powers on the sputtering by 540 keV $C_{60}^{2+}$ ions was performed based on the i-TS model. The obtained result roughly explains the observed large sputtering yield.

Acknowledgement

The authors are grateful to the crew of the 400-kV ion implanter at JAEA/Takasaki, which was used for the irradiation of $C_{60}^{2+}$. This work was supported by Grant-in-Aid for Exploratory Research from JSPS (Grant Number 24651114).

**References**

[1] L.E. Seiberling, C.K. Meins, B.H. Cooper, J.E. Griffith, M.H. Mendenhall, T.A. Tombrello, Nucl. Instr. and Methods in Phys. Res. B **198** (1982) 17.

[2] W. Assmann, M. Toulemonde and C. Trautmann, in *Sputtering by Particle Bombardment* eds. R. Behrisch and W. Eckstein Springer-Verlag Berlin Heidelberg 2007.

[3] M. Toulemonde, W. Assmann, C. Trautmann and F. Gruner, Phys. Rev. Lett. 88 (2002) 057602.

[4] I.A. Baranov, Yu.V. Martynenko, S.O. Tsepelevich, Yu.N. Yavlinskii, Sov. Phys. Usp. **31** (1988) 1015.

[5] T.A. Tombrello, Nucl. Instr. and Methods in Phys. Res. B **2** (1984) 555.

[6] K. Wien, Radiat. Eff. And Def. Sol. **109** (1989) 137.

[7] R.A. Baragiola, Phil. Trans. R. Soc. A **362** (2004) 29.

[8] R.L. Fleischer, P.B. Price and R.M. Walker, J. Appl. Phys. **36** (1965) 3645.

[9] I.S. Bitensky, A.M. Goldenberg and E.S. Parilis, Methods and Mechanisms for Producing Ions from Large Molecules, eds. K.G. Standing and W. Ens (Plenum, New York, 1991) p. 83.

[10] R.E. Jphnson, B.U.R. Sundqvist, A. Hedin and D. Fenyö, Phys. Rev. B **40** (1989) 49.

[11] P.K. Haff, Appl. Phys. Lett. **29** (1976) 473.

[12] K. Nakajima Y. Morita, M. Suzuki, K. Narumi, Y. Saitoh, N. Ishikawa, K. Hojou, M. Tsujimoto, S. Isoda and K. Kimural, Nucl. Instr. and Methods in Phys. Res. B **291** (2012) 12.

[13] Y. Morita, K. Nakajima, M. Suzuki, K. Narumi, Y. Saitoh, N. Ishikawa, K. Hojou, M. Tsujimoto, S. Isoda and K. Kimura, Nucl. Instr. and Methods in Phys. Res. B in press.

[14] K. Kimura, S. Joumori, Y. Oota, K. Nakajima, and M. Suzuki, Nucl. Instr. and Methods in Phys. Res. B **219-220** (2004) 351.

[15] Q. Yang, D.J. O'Connor and Z. Wang, Nucl. Instr. and Methods in Phys. Res. B **61** (1991) 149.

[16] J.F. Ziegler, J.P. Biersack, U.L. Littmark, The Stopping and Range of Ions in Solids, Pergamon Press, New York, 1985.

[17] K. Narumi *et al*, in preparation

[18] W.M. Arnoldbik, N. Tomozeiu, F.H.P.M. Habraken, Nucl. Instrum. Methods in Phys. Res. B 203 (2003) 151.

[19] D.D.N. Barlo Daya, A. Hallén, J. Eriksson, J. Kopniczky, R. Papaléo, C.T. Reimann, P. Håkansson, B.U.R. Sundqvist, A. Brunelle, S. Della-Negra and Y.Le Beyec, Nucl. Instr. and Methods in Phys. Res. B **106** (1995) 38.

[20] M. Toulemonde, W.J. Weber, G. Li, V. Shutthanandan, P. Kluth, T. Yang, Y. Wang and Y. Zhang, Phys. Rev. B **83** (2011) 054106.

[21] C. T. Reimann, Nucl. Instr. and Methods in Phys. Res. B **95** (1995) 181.

**Figure captions**

Fig. 1 TEM bright field images of a-$Si_3N_4$ film (20 nm) irradiated with 540 keV $C_{60}^{2+}$ ions to a fluence of ~ 2 ×$10^{11}$ ions/$cm^2$. The TEM images taken at a tilt angle of (a) 0° and (b) 25° are shown.

Fig. 2 HRBS spectra of virgin a-SiN(30 nm)/Si(001). The <111> channeling spectrum (circles) and the random spectrum (triangles) observed at scattering angle ~75° are shown. The arrows indicate the leading edge positions calculated for Si, O, N and C.

Fig. 3 Composition depth profiles derived from the observed HRBS spectra. The results before and after the irradiation of 540 keV $C_{60}^{2+}$ ions to a fluence of 2.3 × $10^{13}$ ions/$cm^2$ are shown.

Fig. 4 <111> channeling spectra of a-SiN/Si(001) irradiated at various fluences. The spectra are vertically shifted for clarify. The dashed lines show the estimated silicon spectra.

Fig. 5 Areal densities of Si and N atoms in the a-SiN film as a function of the fluence of $C_{60}^{2+}$.

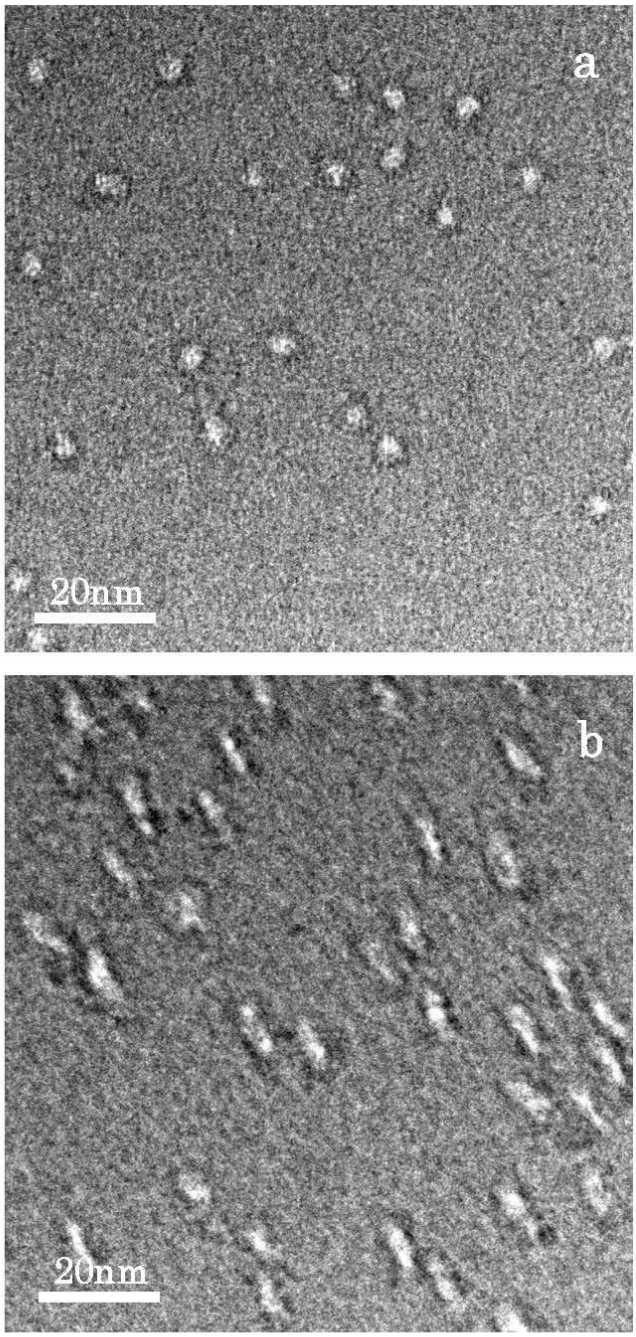


**Fig. 1 K. Nakajima et al**

1

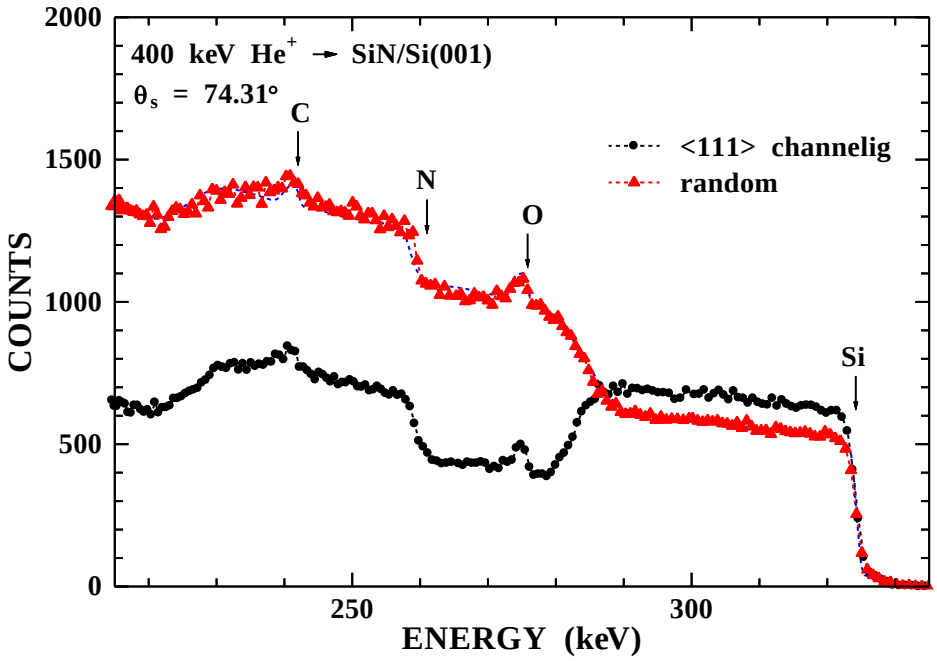


Fig 2 K. Nakajima et al

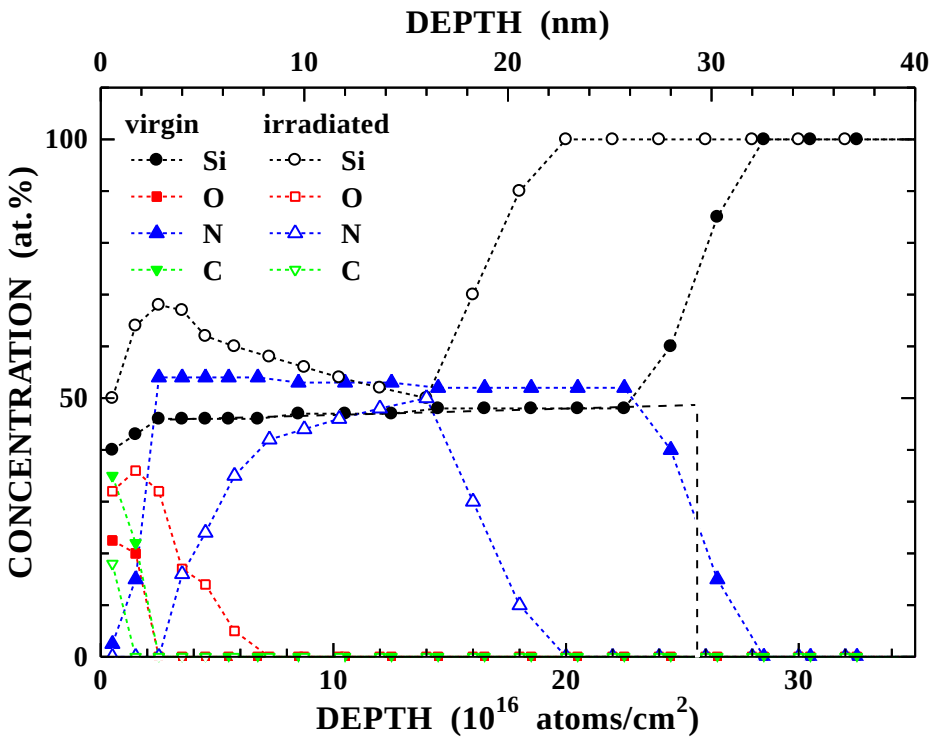


Fig. 3 K. Nakajima et al

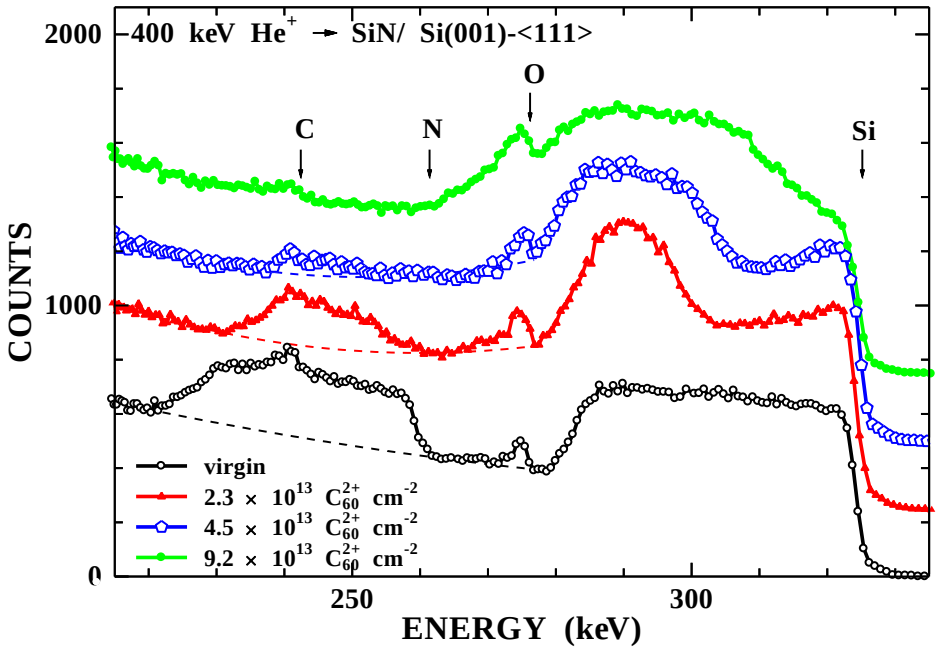


Fig 4 K. Nakajima et al

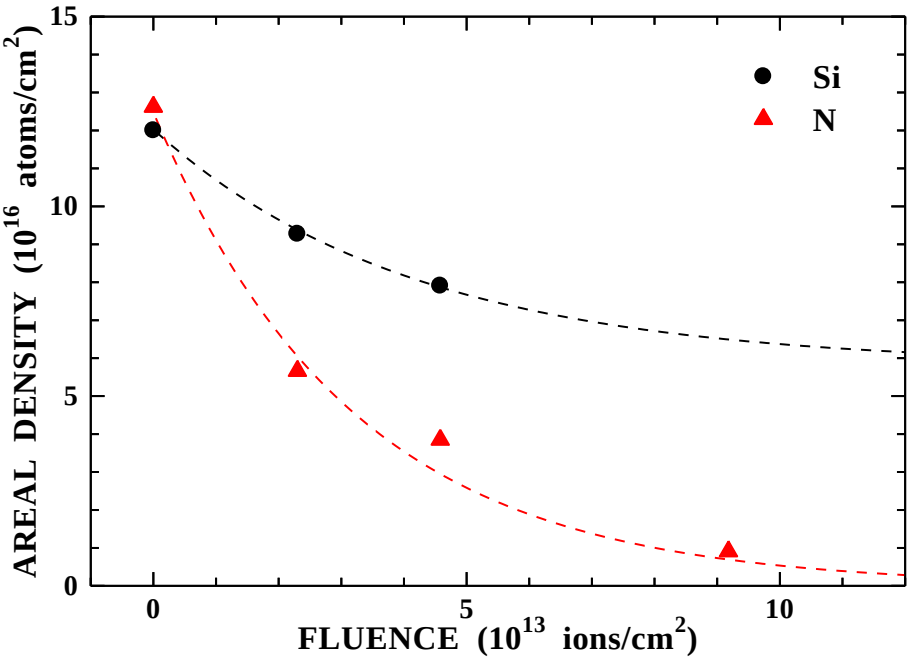


Fig. 5 K. Nakajima et al